



CAIPIRINHA-accelerated 10-min 3D TSE MRI of the ankle for the diagnosis of painful ankle conditions: Performance evaluation in 70 patients

Benjamin Fritz^{1,2} · Susanne Bensler^{1,2} · Gaurav K. Thawait³ · Esther Raithel⁴ · Steven E. Stern⁵ · Jan Fritz³

Received: 13 March 2018 / Revised: 19 May 2018 / Accepted: 4 June 2018 / Published online: 23 July 2018
© European Society of Radiology 2018

Abstract

Objectives To test the hypothesis that MRI of the ankle with a 10-min 3D CAIPIRINHA SPACE TSE protocol is at least equivalent for the detection of painful conditions when compared to a 20-min 2D TSE standard of reference protocol.

Methods Following institutional review board approval and informed consent, 70 symptomatic subjects underwent 3T MRI of the ankle. Six axial, sagittal and coronal intermediate-weighted (IW) and fat-saturated T2-weighted (T2FS) 2D TSE (total acquisition time, 20 min), and two sagittal isotropic IW and T2FS 3D CAIPIRINHA TSE (10 min) pulse sequence prototypes were obtained. Following randomization and anonymization, two musculoskeletal radiologists evaluated the 2D and 3D datasets independently. Descriptive statistics, inter-reader reliability, inter-method concordance, diagnostic definitiveness tests were applied. *P*-values < 0.05 were considered significant.

Results Readers diagnosed 116 cartilage defects with 2D and 109 with 3D MRI, 35 ligament tears with 2D and 65 with 3D MRI, 18 tendon tears with 2D and 20 with 3D MRI, and 137 osseous abnormalities with 2D and 149 with 3D MRI. The inter-reader agreement was high for 2D (Kendall W, 0.925) and 3D MRI (W, 0.936) (*p* < 0.05), as was the inter-method concordance (W, 0.919). The diagnostic definitiveness of readers was higher for 3D MRI than 2D MRI in 10–27% of the time, while the reverse was true in 7–11% of the time (*p* < 0.01).

Conclusions The performance of 10-min 3D CAIPIRINHA SPACE MRI for the detection of painful ankle conditions is similar to that of a 20-min 2D TSE MRI reference standard.

Key Points

- CAIPIRINHA Acceleration facilitates isotropic 3D MRI of the Ankle in 10 min.
- 10-min 3D CAIPIRINHA MRI and 20-min 2D TSE MRI have similar performance.
- 3D CAIPIRINHA SPACE MRI afforded higher diagnostic definitiveness of readers.

Keywords Ankle joint · Magnetic resonance imaging · Imaging · Three-dimensional · Acceleration

✉ Jan Fritz
jfritz9@jhmi.edu

¹ Radiology, Balgrist University Hospital, Zurich, Switzerland

² Faculty of Medicine, University of Zurich, Zurich, Switzerland

³ Russell H. Morgan Department of Radiology and Radiological Science, Section of Musculoskeletal Radiology, Johns Hopkins University School of Medicine, 601 N. Caroline Street, JHOC 3140A, Baltimore, MD 21287, USA

⁴ Siemens Healthcare GmbH, Allee am Roethelheimpark 2, 91052 Erlangen, Germany

⁵ Bond Business School, Bond University, QLD, Gold Coast 4229, Australia

Abbreviations

2D	Two-dimensional
3D	Three-dimensional
CAIPIRINHA	Controlled aliasing in parallel imaging results in higher acceleration
IW	Intermediate-weighted
MRI	Magnetic resonance imaging
SPACE	Sampling perfection with application optimized contrast using different flip angle Evolution
T2FS	Fat-suppressed T2-weighted
TSE	Turbo spin echo

Introduction

Magnetic resonance imaging (MRI) of the ankle is frequently used to investigate pain of unknown origin and characterization of painful conditions [1–4]. The complexity of the ankle anatomy with oblique orientations of numerous cartilaginous, ligamentous and tendinous structures [5–7] often requires multiple planes when using two-dimensional (2D) TSE techniques. In contrast, three-dimensional (3D) TSE techniques can acquire isotropic data sets that are capable of axial, sagittal, coronal, oblique and curved planar reformations from single datasets to optimize the display of ankle structures [7–10].

Despite these favorable attributes, 3D TSE techniques thus far have required trade-offs between long acquisition times, edge blurring, limited anatomical coverage and sub-optimal image contrast [8, 11–14]. The implementation of a CAIPIRINHA (Controlled Aliasing In Parallel Imaging Results IN Higher Acceleration) sampling pattern with a shifted, bi-directional, two-fold accelerated, parallel imaging scheme into 3D SPACE (Sampling Perfection with Application optimized Contrast) TSE remedies many of the shortcomings by affording higher accelerations factors,

image contrast and quality similar or better to 2D TSE images, minimized aliasing artifacts and reduced image noise [15, 16].

The purpose of our study was to test the hypothesis that MRI of the ankle with a 10-min 3D CAIPIRINHA SPACE TSE protocol is at least equivalent for the detection of painful conditions when compared to a 20-min 2D TSE standard of reference protocol.

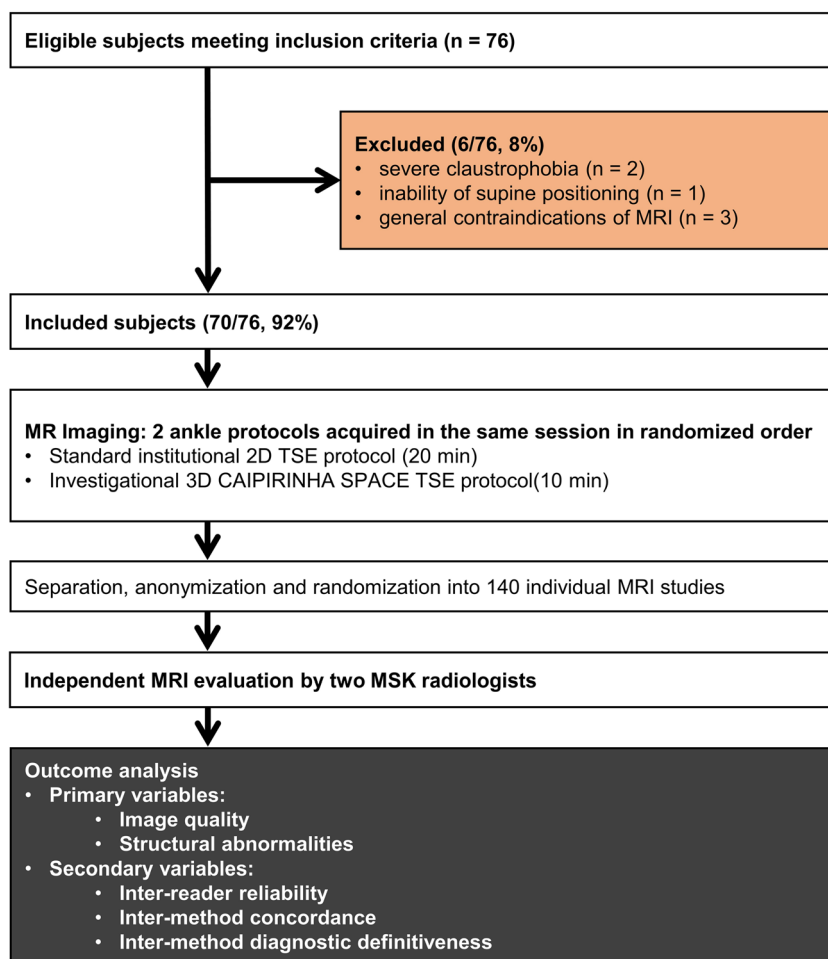
Material and methods

Study design

Our institutional review board approved our study. Written informed consent was obtained from all patients for prospective data collection and use of investigational pulse sequences. None of the patients included in this study have been previously reported.

We recruited patients from our orthopedic practice who presented with painful ankle conditions that met the criteria for ankle MRI [17, 18]. Inclusion criteria were

Fig. 1 Study design



an agreement to participate in our study and adult age. Exclusion criteria were a degree of ankle swelling preventing positioning into an ankle coil, inability for supine positioning, severe claustrophobia and general contraindications for MRI (Fig. 1). All subjects underwent MRI of the ankle in one session using both, our standard 2D TSE MRI pulse sequence protocol and investigational 3D TSE prototype protocol (Table 1).

Subjects

Between January 2016 and June 2016, 70 subjects (46 men, 24 women; mean age, 42 years, range: 18–72 years; mean body mass index, 27 kg/m², range: 18–35 kg/m²) were prospectively included for unilateral MRI of the ankle.

MR imaging technique

All MRI exams were performed on a commercially available, clinical wide-bore 3 Tesla MR imaging system (MAGNETOM Skyra, Siemens Healthcare, Erlangen, Germany) with a commercially available boot-shaped foot and ankle surface coil with one transmit channel and 16 receiver channels (Siemens Healthcare). All subjects underwent the MRI study protocol with a total acquisition time of 30 min, which consisted of a 3D TSE pulse sequence protocol with an acquisition time of 10 min and a 2D TSE pulse sequence protocol with an acquisition time of 20 min (Table 1). Either the 2D or 3D protocol portion was acquired first with equal proportions throughout the study. The investigational 3D protocol was based on a 2 x 2-accelerated 3D SPACE TSE sequence prototype that utilized a shifted, bi-directional parallel imaging and CAIPIRINHA sampling pattern [16]. One non-fat-suppressed intermediate-weighted (IW) and one fat-suppressed T2-weighted (T2FS) 3D CAIPIRINHA SPACE TSE dataset with isotropic voxel resolution were acquired. Our institutional 2D TSE protocol for MRI of the ankle served as the standard of reference, which is characterized by fully sampled data sets without undersampling or acceleration techniques to ensure the highest image quality. All sagittal 2D and 3D TSE pulse sequences were aligned to the anteroposterior axis of the talus and rotated 45° in the sagittal plane, which resulted in an anterosuperior to the posteroinferior in-plane phase-encoding direction across the ankle that obviated the use of phase oversampling. The final images were digitally rotated back on the MRI console immediately after completing the pulse sequence. To avoid phase wrap artefacts in the slice partition direction, the contralateral ankle was either elevated above the surface coil or pulled back to reside proximal to the surface coil.

Table 1 MRI study protocol

Parameters	2D MRI protocol		3D MRI protocol	
	Intermediate-weighted 2D TSE	T2-SPAIR 2D TSE	Intermediate-weighted 3D CAIPIRINHA SPACE	T2-SPAIR 3D CAIPIRINHA SPACE
Orientation	Axial	Axial	Sagittal	Sagittal
Repetition time (ms)	4,590	4,490	4,030	1,100
Echo time (ms)	33	68	64	110
Echo train length	15	14	13	54
Receiver bandwidth (Hertz/pixel)	381	180	180	422
Field-of-view (mm)	160 x 160	160 x 160	160 x 160	160 x 160
Voxel dimensions (mm)	0.5 x 0.5 x 3.0	0.5 x 0.5 x 3.0	0.5 x 0.5 x 2.7	0.5 x 0.5 x 0.5
Number of Slices	45	45	34	176
In-plane frequency encoding direction	right-to-left	right-to-left	right-to-left	anterior-to-posterior
Acquisition time	3 min 39 s	3 min 54 s	3 min 42 s	4 min 46 s
			anterior-to-posterior	anterior-to-posterior
			3 min 14 s	5 min 10 s

TSE turbo spin echo, CAIPIRINHA Controlled aliasing in parallel imaging results in higher acceleration, SPACE Sampling perfection with application optimized contrast using different flip angle Evolution

Table 2 Qualitative assessment

Rating	Degree of motion	Image quality	Description
1	Non-diagnostic	Non-diagnostic	Complete non-visibility of anatomical details
2	Severe	Bad	Severely impaired visibility of anatomical details
3	Moderate	Moderate	Impaired visibility of only fine anatomical detail
4	Mild	Good	Minimal impaired visibility, but preservation of all anatomical detail
5	None	Very good	Unimpaired visibility of all anatomical details

Image evaluation

The 70 pairs of 2D and 3D TSE datasets were separated, anonymized and randomized, resulting in 140 individual studies. Each of those 140 studies was evaluated by two fellowship-trained, full-time musculoskeletal radiologists, with 5 years and 10 years of experience in interpreting musculoskeletal MRI examinations, respectively. Each reader evaluated the studies independently. Before the evaluation, both readers underwent a joint training session with 15 complete studies that were not included in our study. Readings were performed in a standardized condition [19]. All data sets were displayed with a 2 x 3 viewport layout. For 2D TSE, individual image stacks were displayed, whereas 3D data sets were displayed using the interactive multiplanar reformation mode of the viewer software with the original isotropic voxel size (MERLIN Diagnostic Workcenter, Phönix-PACS GmbH).

Outcome variables

Variables included the degree of motion, overall image quality defined as the reader's subjective impression of the suitability of the study for accomplishing an MRI interpretation of the ankle, frequency of structural abnormalities, inter-reader reliability defined as the degree of agreement between the two readers for assessments made, inter-method concordance defined as the degree of agreement of readers' diagnoses between corresponding 2D and 3D studies, diagnostic definitiveness defined as the degree of readers' certainty for diagnoses, and interchangeability defined as common pair exact match proportions between readers of different combinations of 2D and 3D studies [20].

For the assessments of the degree of motion and overall image quality, equidistant 5-point Likert scales were used (Table 2).

For evaluation of the frequency of structural abnormalities, a total of nine bones, six joints, 12 ligaments and ten tendons were assessed. Bones were assessed for fractures, bone marrow edema or both, whereas tendons and ligaments were assessed for tears, using an equidistant 5-point Likert-scale as certainly not, probably not, equivocal, probably yes and certainly yes. A fracture was defined as discontinuity of cortical bone or a sharp hypointense osseous line on IW and T2FS images with surrounding bone marrow edema. Bone marrow edema was defined as ill-defined osseous signal hyperintensity on T2FS images. Tears were defined as greater than 50% short-axis fibre disruption and long-axis splits. Each joint was evaluated separately for the absence (modified Noyes grade 0 and 1) or presence (grade 2 and 3) of cartilage defects [21, 22]. In addition, each reader rated their level of confidence as less than 50%, 50–90% and > 90% certainty.

Statistical analysis

Statistical analyses were performed using R version 3.3 with the lme4 and epiR packages (<http://cran.r-project.org>). Motion and diagnostic quality assessments are given as the median value with minimum, first–third quartile and maximum, and the chi-squared test was used to test for reader differences. For the analysis of frequencies and proportions, reader responses were dichotomized into 'present' (for certainly yes and probably yes) or 'absent' (equivocal, probably no and certainly no). All assessments were performed on a location-by-location basis; for example, for cartilage defects

Table 3 Frequency of structural abnormalities and inter-reader reliability

Structure	2D TSE			3D TSE			Combined		
	Reader 1	Reader 2	Kendall's W	Reader 1	Reader 2	Kendall's W	2D TSE	3D TSE	McNemar's <i>p</i> -value
Cartilage	76/420 (18%)	156/420 (37%)	0.901	102/420 (24%)	116/420 (28%)	0.958	116/420 (27%)	109/420 (26%)	<i>p</i> = 0.440
Ligament	33/840 (4%)	39/840 (5%)	0.657	59/840 (7%)	71/840 (8%)	0.778	36/840 (4%)	65/840 (8%)	<i>p</i> < 0.001
Tendon	14/630 (2%)	21/630 (3%)	0.672	18/630 (3%)	22/630 (3%)	0.786	18/630 (3%)	20/630 (3%)	<i>p</i> = 0.125
Bone	130/630 (21%)	130/630 (21%)	0.948	139/630 (22%)	136/630 (22%)	0.956	133/630 (21%)	138/630 (22%)	<i>p</i> = 0.729

TSE turbo spin echo

the same joint had to have a defect to be considered as having an agreement. Differences in the frequencies of structural abnormalities on 2D and 3D MRI were tested with McNemar's test. Inter-reader reliability of measurements was assessed with the exact agreement and Kendall's coefficient of concordance, W using dichotomized data. Kendall's coefficient of concordance, W was qualified into poor (0–0.20), fair (0.21–0.40), moderate (0.41–0.60), good (0.61–0.80) and very good (0.81–1.00), paralleling the criteria that were defined for Cohen's kappa [23]. The degree of concordance between 2D and 3D TSE assessments was assessed with dichotomized average reader values due to a high degree of inter-reader reliability using exact agreement and Kendall's coefficient of concordance, W . The diagnostic definitiveness was used to describe the proportion of times that a common diagnosis was given more strongly after evaluation of 2D TSE or 3D TSE images, whereas cases with a discrepant finding between 2D and 3D images were excluded for this part of the analysis.

For comparison of diagnostic definitiveness of each MRI technique, average reader values were used to describe the proportions of certainty levels of 2D and 3D MRI in the case of an agreement on the presence or absence. Interchangeability of 2D and 3D techniques for diagnoses of structural abnormalities was assessed with likelihood ratio testing, using proportions of exact matches when both readers were reading 2D studies, one reader was reading 2D TSE and one 3D studies, and both readers were reading 3D studies and final testing for significant differences. P -values of less than 0.05 were considered statistically significant.

Results

There was no substantial motion degradation of either 2D TSE (5 [2, 5]) or 3D TSE (5 [4, 5]) studies ($p = 0.368$), with very good inter-reader agreement (Kendall W , 0.889).

Fig. 2 A 57-year-old man with chronic right heel pain. Sagittal intermediate-weighted 2D (a) and 3D (b) MR images and sagittal fat-suppressed T2-weighted 2D (c) and 3D (d) MR images show an insertional partial-thickness tear of the Achilles tendon (white arrow), fluid in the retrocalcaneal bursa (asterisk) and intra-ligamentous heterotopic ossification (grey arrow)



3D TSE studies had non-significantly ($p = 0.441$) higher image quality ratings (5 [2, 4, 5]) than 2D TSE studies (4 [3, 5]), with very good inter-reader agreement (Kendall W, 0.816). The average ratings for the overall image quality for 3D TSE exceeded the rating of 2D TSE in 51/70 (73%) of cases, whereas the overall image quality ratings for 2D TSE exceeded the rating of 3D TSE in 5/70 cases (7%).

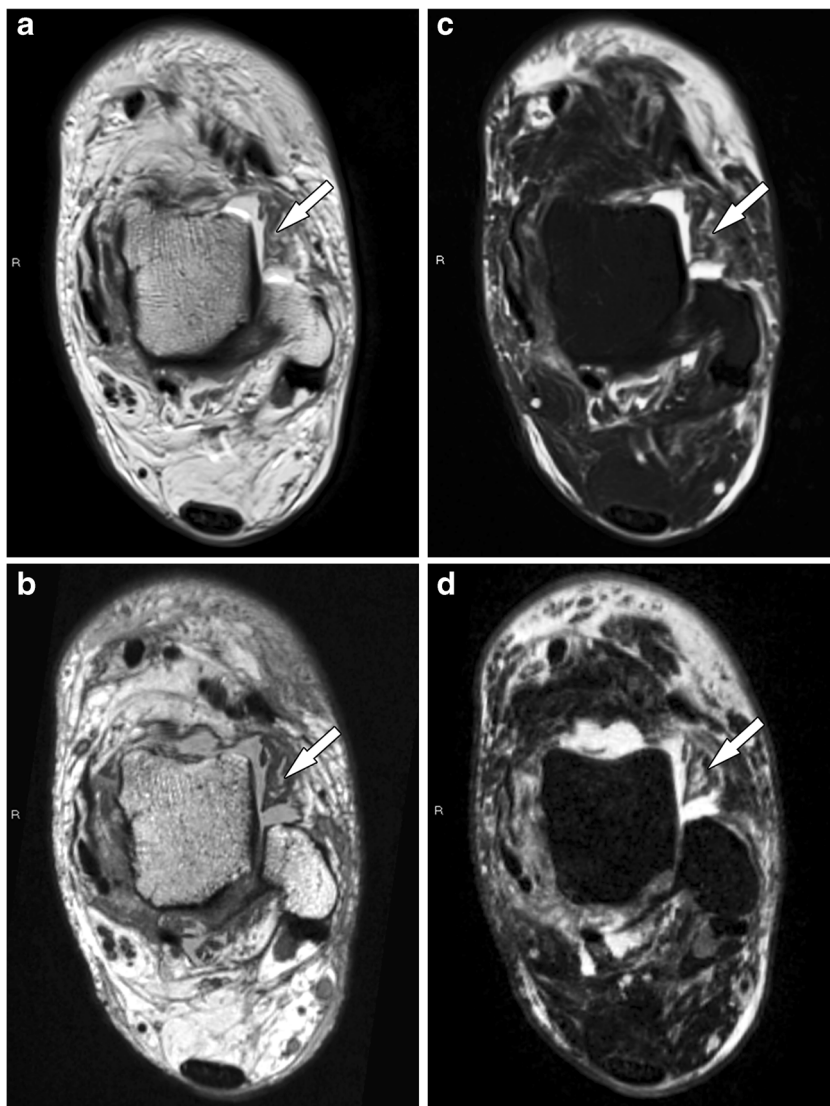
The frequencies for the detection of structural abnormalities and inter-reader reliabilities are given in Table 3, which are based on the total number of 420 cartilage segments, 840 ligaments, 630 tendons and 630 bones (Figs. 2, 3, 4, 5 and 6). Reader 1 diagnosed 6% fewer and reader 2 diagnosed 9% more cartilage defects with 2D MRI when compared to 3D MRI. In-between readers, the difference of frequencies of cartilage lesions was 19% for 2D MRI and 4% for 3D MRI ($p < 0.001$). The overall difference between 2D and 3D MRI for the diagnosis of cartilage lesions was 1%, which includes normal cartilage diagnoses ($p = 0.440$). Both readers detected

3% more ligament tears with 3D MRI than 2D MRI ($p < 0.001$), while the detection rate differences of tendon tears ($p = 0.125$) and osseous bone abnormalities ($p = 0.729$) were 0–1%. Overall, there was very good inter-reader agreement for 2D MRI (Kendall W, 0.925; range, 0.657–0.948) and 3D MRI (Kendall W, 0.936; range, 0.778–0.958).

There was overall very good inter-method concordance (Kendall W, 0.919; range, 0.732–0.947) between 2D and 3D MRI, with the highest concordance for osseous abnormalities and lowest concordance for ligamentous injuries (Table 4).

The diagnostic definitiveness of readers for cartilage assessments was higher for 3D MRI than 2D MRI 27% of the time, while the reverse was true 11% of the time. Table 5 presents the diagnostic definitiveness for ligaments, tendons and bones as the proportion of times the confidence of 3D TSE reader responses exceeded the 2D TSE reader responses and vice versa for the cases where both readers agreed on the presence or absence of findings. For the assessments of

Fig. 3 A 34-year-old man with acute left ankle inversion-type injury. Axial intermediate-weighted 2D (a) and 3D (b) MR images and axial fat-suppressed T2-weighted 2D (c) and 3D (d) MR images show a complete tear of the anterior talofibular ligament (arrow)



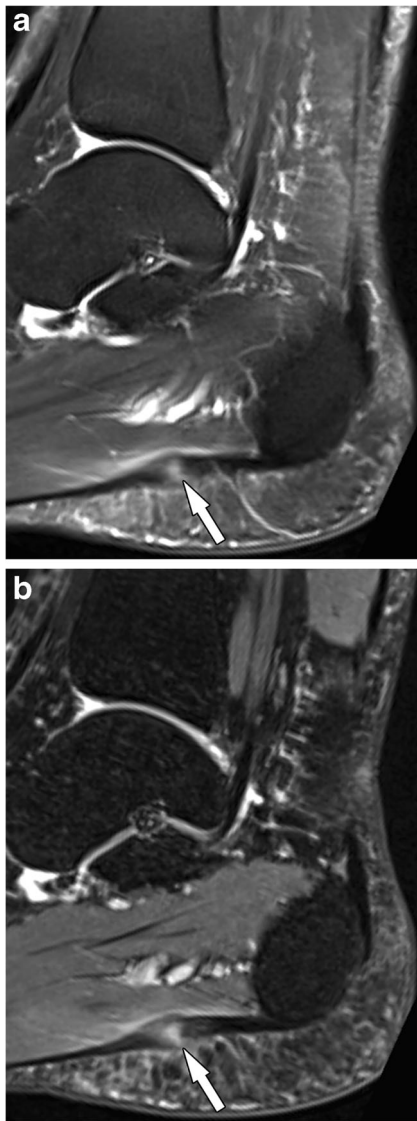


Fig. 4 A 42-year-old woman with chronic plantar pain. Sagittal fat-suppressed T2-weighted 2D (a) and 3D (b) MR images show a non-insertional tear of the central cord of the plantar fascia (arrow) on a background of focal fibrosis

ligaments, tendons and bones, the confidence of 3D reader responses exceeded the 2D reader response in 10% of cases, whereas the confidence of 2D reader responses exceeded the 3D reader response in 7% of cases ($p < 0.01$). The proportions of excluded cases on which both readers disagreed on the diagnosis on 2D and 3D images were 5.5% for ligaments, 1.4% for tendons, 5.5% for bones and 4.2%.

The interchangeability analysis (Table 6) shows that the common pair exact match proportions were similar between 2D and 3D studies when readers diagnosed bone abnormalities, which indicates bi-directional interchangeability of 2D and 3D technique. The common pair exact match proportions were significantly higher ($p < 0.05$) for the 3D technique when readers diagnosed abnormalities of cartilage, ligaments and tendons, indicating higher internal reliability of the 3D

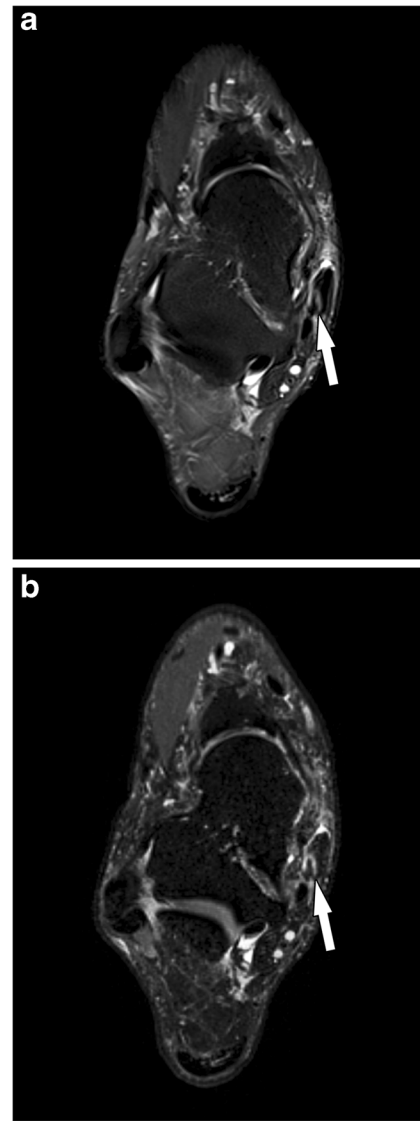


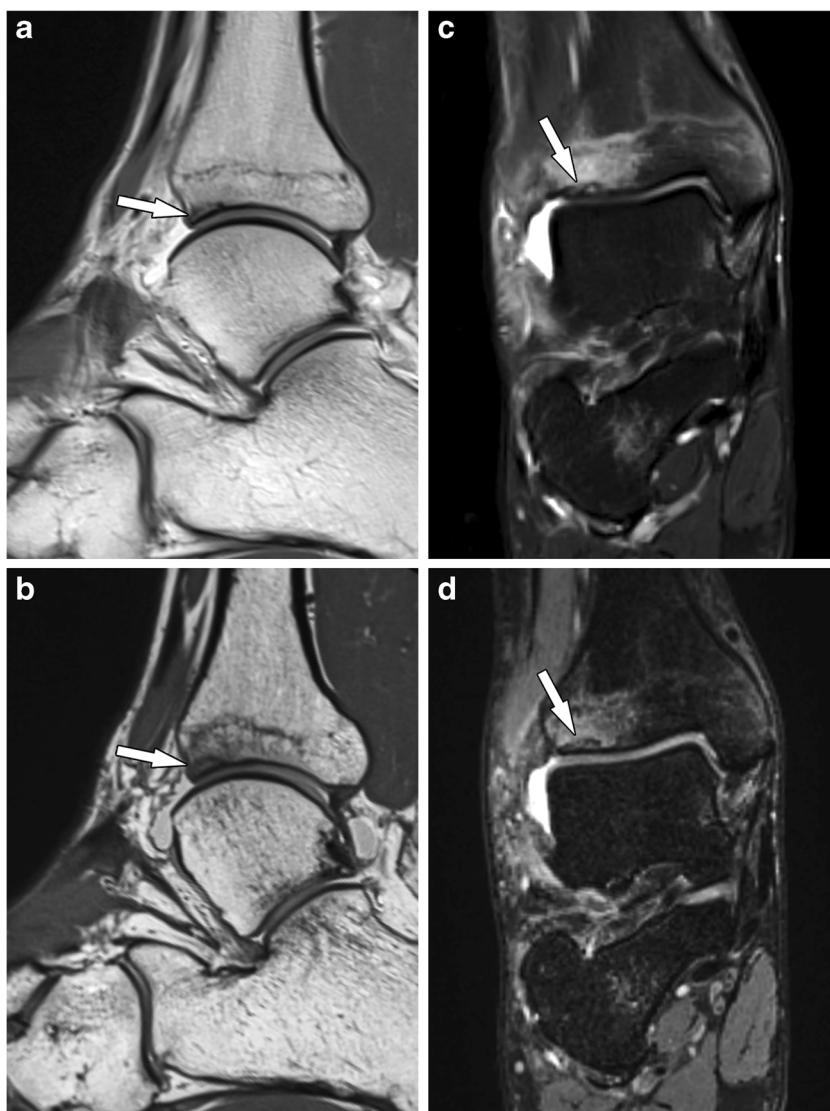
Fig. 5 A 55-year-old woman with chronic medial ankle pain. Axial fat-suppressed T2-weighted 2D (a) and 3D (b) MR images show a split tear of the posterior tibial tendon (arrow)

technique and unidirectional interchangeability, meaning that only the 3D technique can replace the 2D technique.

Discussion

We compared a novel 10-min 3D CAIPIRINHA SPACE TSE protocol to a 2D TSE standard of reference protocol for the diagnosis of painful ankle conditions. Readers detected more ligament tears with 3D than 2D MRI, while the overall differences for cartilage, tendons and osseous abnormalities were small. The inter-method concordance and inter-reader reliability were overall high, whereas the diagnostic definitiveness and internal reliability were higher for 3D CAIPIRINHA SPACE TSE than 2D TSE images, indicating that the 3D CAIPIRINHA

Fig. 6 A 27-year-old man with an acute ankle injury. Sagittal intermediate-weighted 2D (a) and 3D (b) MR images and coronal fat-suppressed T2-weighted 2D (c) and 3D (d) MR images show a non-displaced, subchondral fracture (arrow) of the anterior tibial plafond



SPACE TSE protocol is at least equivalent and can replace the 2D technique for the detection of painful ankle conditions.

Owing to rising economic constraints and the demand of MRI for non-invasive diagnosis of painful ankle conditions, there is a need for faster MRI acquisition without comprising diagnostic accuracy. 10-minute MRI of the ankle offers short

Table 4 Inter-method concordance between 2D and 3D MRI

Structure	Exact match*	Kendall's W
Cartilage	80.0%	0.784
Ligament	93.1%	0.732
Tendon	96.1%	0.810
Bone	92.8%	0.847
Overall	91.9%	0.919

*Proportion of exact matches of reader assessments of corresponding to 2D and 3D MRI

table times for patients and can contribute to a high institutional throughput and potentially compensate for decreasing reimbursements. The 10-min acquisition time of our 3D TSE protocol was mainly based on a 2 x 2 acceleration with a shifted, bi-directional CAIPIRINHA undersampling in phase and partition encoding directions [24, 25]. This approach optimized the use of coil sensitivities, which helped to minimize aliasing artefacts and reduce image noise [16]. The isotropic 3D TSE voxel size allowed for the interactive reformation of the standard axial, sagittal and coronal as well as oblique planes.

When compared to 2D TSE, the higher spatial resolution that is achievable with 3D TSE pulse sequences relates to signal gains from volume, rather than slice selective excitations, and the number of additional phase-encoding steps of the slice partitions. However, the number of slice partitions results in longer acquisition times, which can range between 20 and 30 min for fully sampled data sets. Applying different

Table 5 Diagnostic definitiveness

Diagnostic outcome	Ligaments		Tendons		Bones		Combined	
	3D > 2D*	3D < 2D**	3D > 2D	3D < 2D	3D > 2D	3D < 2D	3D > 2D	3D < 2D
Presence	67%	5%	59%	6%	15%	4%	28%	4%
Absence	16%	13%	8%	5%	5%	4%	9%	7%
All	17%	13%	10%	5%	6%	4%	10%	7%

*3D > 2D: proportion of times the confidence of 3D TSE reader responses exceeded the 2D TSE reader response for a common diagnosis that was given after evaluation of 2D TSE or 3D TSE images

**2D > 3D: proportion of times the confidence of 3D TSE reader responses exceeded the 2D TSE reader response for a common diagnosis that was given after evaluation of 2D TSE or 3D TSE images

acceleration strategies and techniques, previous 3D TSE studies investigating high-resolution MRI of the ankle reported acquisition times of 5–8 min for a single 3D TSE dataset [8, 9, 13, 14, 26, 27]. Applied strategies included long echo train lengths of up to 100 [13, 14, 26], anisotropic voxel size acquisitions [14, 27], in-directional parallel imaging acceleration of up to three [8, 13] and partial Fourier undersampling [8, 9, 13, 26], which are all inversely proportional to the acquisition times. While those techniques in combination can mathematically achieve net accelerations of three to six, they result in various but often meaningful degradation of image quality including decreased signal-to-noise ratios, increased image blurring and aliasing artefacts. Additional strategies to reduce the acquisition time included limited field-of-view dimensions and a reduced number of slice-encoding partitions that cover specific structures selectively, rather than the entire ankle [8, 13, 26].

The bi-directional acceleration scheme of the 3D CAIPIRINHA SPACE pulse sequence prototype affords a fourfold acceleration through parallel imaging without degrading noise levels or aliasing artefacts [15]. The afforded reduction of acquisition time allowed us to limit the echo train length to 42 and 54 to minimize image blurring, acquire truly isotropic voxels to prevent degrading extrapolation effects and avoid partial Fourier undersampling in both phase-encoding directions, which degrade image quality to various degrees. Additionally, we could realize whole ankle coverage with a sagittal plane field-of-view of 16 x 16 cm, which extended

from the muscle-tendon junction of the Achilles tendon to the midfoot, and mediolateral skin-to-skin coverage of 9 cm, providing identical coverage than our 2D TSE protocol. Lastly, driven equilibrium pulse technique to restore the longitudinal magnetization, low repetition times of 1,000 and 1,100 ms, and the use of elliptical k-space sampling resulted in additional time savings [16].

Previous studies have suggested equal or better visualization capabilities of 3D TSE MRI of the ankle for cartilage lesions as well as tendon and ligament tears when compared to 2D TSE ankle MRI [8, 9, 13, 14, 16, 26, 27]. Our study showed a high inter-method concordance for the detection of abnormalities, whereas the inter-reader reliability was higher for 3D TSE images. For evaluation of cartilage lesions, however, there was a notable discrepancy between readers. Reader 1 detected fewer and reader 2 detected more cartilage lesions with 2D than 3D MRI, whereas the inter-reader reliability was notably higher for 3D images. On the other hand, both readers detected more ligament tears with 3D than 2D MRI with overall low inter-reader reliability, but higher for 3D MRI. While the lower 2D inter-reader reliability for diagnosing cartilage defects may relate to different sensitivity levels of the readers, the thin articular cartilage layers of the ankle and a lack of robustly designed cartilage grading systems with previously reported low inter-reader reliabilities were likely contributing factors [28]. The high inter-reader reliability and diagnostic definitiveness of 3D TSE for both cartilage lesions and ligament tears suggest an advantage of 3D TSE. The 3D CAIPIRINHA SPACE pulse sequence is Conformité Européenne marked and received US Food and Drug Administration 510(k) clearance. Following a transition period of acquiring both 2D and 3D techniques, we have since replaced our conventional 2D protocol with the new 3D protocol for MRI of the ankle at the Johns Hopkins Medical Institutions.

Similar to our results, improved detectability of syndesmotic and lateral collateral ligaments tears on 3D TSE images has been suggested before [9, 14, 27], which likely relates to limited partial volume effects and the ability for interactively align image planes to obliquely oriented ligaments. As multi-dimensional image plane rotation is currently a standard interactive feature of

Table 6 Interchangeability analysis

Diagnostic outcome	Cartilage	Ligaments	Tendons	Bone
% 2D/2D	73.8	78.6	88.0	96.3*
% 2D/3D	78.1	77.9	89.0	87.9
% 3D/3D	91.2**	82.7**	92.3**	96.6**

*2D/2D common pair exact match proportions are statistically significantly different from 2D/3D common pair exact match mixed proportions

**3D/3D common pair exact match proportions are statistically significantly different from 2D/3D pair exact match mixed proportions

professional image viewers, the additional time required to perform these tasks is small. Therefore, we believe that replacing an existing 2D TSE protocol with the more time-efficient 3D CAIPIRINHA SPACE TSE protocol is feasible in a clinical setting and can be recommended for the purpose of reducing scan time without degrading image quality and detection of structural abnormalities.

Our study has limitations. First, there was no standard of reference to confirm the detected anatomical abnormalities. Surgical exploration is often used as a standard of reference when assessing injuries in other joints such as the knee and the hip. In the ankle joint, however, only a few abnormalities, such as osteochondral defects of the talus and complete tendon ruptures, are amenable for a definitive and accurate intra-operative diagnosis, while surgical exploration frequently does not provide a diagnosis of certainty for most of the ligamentous and chronic tendinous ankle injuries. As such, we used statistical metrics to compare both techniques. While this approach can determine equivalence, the superiority of one technique over the other can only be suggested. Second, while both readers were blinded to corresponding 2D and 3D data sets, the differences in the number of slices and spatial resolutions allowed readers to recognize the technique. Therefore, personal preferences may have influenced the study results. Both readers did not, however, use 3D TSE techniques in their daily clinical practice. Third, the novel 3D TSE protocol was compared to our institutional standard 2D TSE protocol for MRI of the ankle. However, MRI ankle protocols vary in part substantially between institutions, and therefore sequences (for example by the inclusion of a T1-weighted pulse sequence), acquisition times and image quality of our study may be different from other established protocols.

In conclusion, a 10-min 3D CAIPIRINHA SPACE MRI protocol produces equal or better image quality and the performance for the detection of painful ankle conditions is similar when compared to a 20-min 2D TSE MRI reference standard. Significantly higher inter-reader reliability and reader definitiveness indicate improved visibility of abnormalities on 3D TSE images, which may have increased accuracy for the detection of ligament tears.

Funding This study has received funding by Siemens AG.

Compliance with ethical standards

Guarantor The scientific guarantor of this publication is Jan Fritz.

Conflict of interest The authors of this paper declare relationships with the following companies: Siemens AG.

Statistics and biometry One of the authors has significant statistical expertise.

Informed consent Written informed consent was obtained from all subjects in this study.

Ethical approval Institutional Review Board approval was obtained.

Methodology

- prospective
- experimental
- performed at one institution

References

1. Rosenberg ZS, Beltran J, Bencardino JT (2000) From the RSNA Refresher Courses. Radiological Society of North America. MR imaging of the ankle and foot. *Radiographics*. 20(Spec No):S153-179
2. Kreitner KF, Ferber A, Grebe P, Runkel M, Berger S, Thelen M (1999) Injuries of the lateral collateral ligaments of the ankle: assessment with MR imaging. *Eur Radiol* 9(3):519–524
3. Cheung Y, Rosenberg ZS (2001) MR imaging of ligamentous abnormalities of the ankle and foot. *Magn Reson Imaging Clin N Am* 9(3):507–531 x
4. Leffler S, Disler DG (2002) MR imaging of tendon, ligament, and osseous abnormalities of the ankle and hindfoot. *Radiol Clin North Am* 40(5):1147–1170
5. Mengiardi B, Pfirmann CW, Vienne P, Hodler J, Zanetti M (2007) Medial collateral ligament complex of the ankle: MR appearance in asymptomatic subjects. *Radiology* 242(3):817–824
6. Mengiardi B, Zanetti M, Schöttle PB et al (2005) Spring ligament complex: MR imaging-anatomic correlation and findings in asymptomatic subjects. *Radiology* 237(1):242–249
7. Duc SR, Mengiardi B, Pfirmann CW, Hodler J, Zanetti M (2007) Improved visualization of collateral ligaments of the ankle: multiplanar reconstructions based on standard 2D turbo spin-echo MR images. *Eur Radiol* 17(5):1162–1171
8. Notohamiprodjo M, Kuschel B, Hornig A et al (2012) 3D-MRI of the ankle with optimized 3D-SPACE. *Invest Radiol* 47(4):231–239
9. Kim M, Choi YS, Jeong MS et al (2017) Comprehensive assessment of ankle syndesmosis injury using 3D isotropic turbo spin-echo sequences: diagnostic performance compared with that of conventional and oblique 3-T MRI. *AJR Am J Roentgenol* 208(4):827–833
10. Hermans JJ, Ginai AZ, Wentink N, Hop WC, Beumer A (2011) The additional value of an oblique image plane for MRI of the anterior and posterior distal tibiofibular syndesmosis. *Skeletal Radiol* 40(1):75–83
11. Notohamiprodjo M, Hornig A, Pietschmann MF et al (2009) MRI of the knee at 3T: first clinical results with an isotropic PDFs-weighted 3D-TSE-sequence. *Invest Radiol* 44(9):585–597
12. Jung JY, Yoon YC, Kwon JW, Ahn JH, Choe BK (2009) Diagnosis of internal derangement of the knee at 3.0-T MR imaging: 3D isotropic intermediate-weighted versus 2D sequences. *Radiology* 253(3):780–787
13. Stevens KJ, Busse RF, Han E et al (2008) Ankle: isotropic MR imaging with 3D-FSE-cube: initial experience in healthy volunteers. *Radiology* 249(3):1026–1033
14. Park HJ, Lee SY, Choi YJ et al (2017) 3D isotropic T2-weighted fast spin echo (VISTA) versus 2D T2-weighted fast spin echo in evaluation of the calcaneofibular ligament in the oblique coronal plane. *Clin Radiol* 72(2):176 e1- e7
15. Fritz J, Fritz B, Thawait GG, Meyer H, Gilson WD, Raithel E (2016) Three-dimensional CAIPIRINHA SPACE TSE for 5-minute high-resolution MRI of the knee. *Invest Radiol* 51(10):609–617
16. Kalia V, Fritz B, Johnson R, Gilson WD, Raithel E, Fritz J (2017) CAIPIRINHA accelerated SPACE enables 10-min isotropic 3D

- TSE MRI of the ankle for optimized visualization of curved and oblique ligaments and tendons. *Eur Radiol* 27(9):3652–3661
17. Mosher TJ, Kransdorf MJ, Adler R et al (2015) ACR Appropriateness Criteria acute trauma to the ankle. *J Am Coll Radiol* 12(3):221–227
 18. DeSmet AA, Dalinka MK, Alazraki N et al (2000) Chronic ankle pain. American College of Radiology. ACR Appropriateness Criteria. *Radiology* 215(Suppl):321–332
 19. Bidgood WD Jr, Horii SC (1992) Introduction to the ACR-NEMA DICOM standard. *Radiographics* 12(2):345–355
 20. Obuchowski NA, Subhas N, Schoenhagen P (2014) Testing for interchangeability of imaging tests. *Acad Radiol*. 21(11):1483–1489
 21. Noyes FR, Stabler CL (1989) A system for grading articular cartilage lesions at arthroscopy. *Am J Sports Med* 17(4):505–513
 22. Kijowski R, Blankenbaker DG, Davis KW, Shinki K, Kaplan LD, De Smet AA (2009) Comparison of 1.5- and 3.0-T MR imaging for evaluating the articular cartilage of the knee joint. *Radiology* 250(3):839–848
 23. Landis JR, Koch GG (1977) The measurement of observer agreement for categorical data. *Biometrics* 33(1):159–174
 24. Breuer FA, Blaimer M, Mueller MF et al (2006) Controlled aliasing in volumetric parallel imaging (2D CAIPIRINHA). *Magn Reson Med* 55(3):549–556
 25. Yutzy SR, Seiberlich N, Duerk JL, Griswold MA (2011) Improvements in multislice parallel imaging using radial CAIPIRINHA. *Magn Reson Med* 65(6):1630–1637
 26. Yi J, Cha JG, Lee YK, Lee BR, Jeon CH (2016) MRI of the anterior talofibular ligament, talar cartilage and os subfibulare: Comparison of isotropic resolution 3D and conventional 2D T2-weighted fast spin-echo sequences at 3.0 T. *Skeletal Radiol* 45(7):899–908
 27. Park HJ, Lee SY, Park NH et al (2016) Three-dimensional isotropic T2-weighted fast spin-echo (VISTA) ankle MRI versus two-dimensional fast spin-echo T2-weighted sequences for the evaluation of anterior talofibular ligament injury. *Clin Radiol* 71(4):349–355
 28. Schmid MR, Pfirrmann CW, Hodler J, Vienne P, Zanetti M (2003) Cartilage lesions in the ankle joint: comparison of MR arthrography and CT arthrography. *Skeletal Radiol* 32(5):259–265